CERN – EUROPEAN ORGANIZATION FOR NUCLEAR RESEARCH

CLIC – Note – 877

DYNAMICS ON THE POSITRON CAPTURE AND ACCELERATING SECTIONS OF CLIC

F. Poirier[2], L. Rinolfi[1], A. Vivoli[1], O. Dadoun[2], P. Lepercq[1], A. Variola[2]
[1]CERN, 1211 Geneva, Switzerland
[2] LAL, IN2P3-CNRS and Université de Paris-Sud, Orsay, France

Abstract

The CLIC Pre-Injector Linac for the e^+ beam is composed of an Adiabatic Matching Device (AMD) followed by 4 (or 5) accelerating RF structures embedded in a solenoidal magnetic field. The accelerating sections are based on 2 GHz long travelling wave structures.
In this note, the positrons capture strategy downstream the AMD is reviewed.
The first RF structure can be phased either for full acceleration or for deceleration. In the latter case, the simulations results show that the number of e^+ capture at the end of the 200 MeV Pre-Injector Linac is increased. Then the impact of the space charge is presented. Additional techniques are also studied to explore the potentiality of increasing the number of e^+ namely an extra RF field at the beginning of the capture section and a higher solenoidal field.

CERN-OPEN-2011-034
23/03/2011

Geneva, Switzerland
July 2011

Dynamics on the positron capture and accelerating sections of CLIC

F. Poirier[2#], L. Rinolfi[1], A. Vivoli[1],
O.Dadoun[2], P Lepercq[2], A. Variola[2],

[1]CERN, 1211 Geneva, Switzerland
[2]LAL, IN2P3-CNRS and Universite de Paris-Sud, 91898, Orsay, France

Abstract

The CLIC Pre-Injector Linac for the e^+ beam is composed of an Adiabatic Matching Device (AMD) followed by 4 (or 5) accelerating RF structures embedded in a solenoidal magnetic field. The accelerating sections are based on 2 GHz long travelling wave structures.
In this note, the positrons capture strategy downstream the AMD is reviewed.
The first RF structure can be phased either for full acceleration or for deceleration. In the latter case, the simulations results show that the number of e^+ capture at the end of the 200 MeV Pre-Injector Linac is increased. Then the impact of the space charge is presented. Additional techniques are also studied to explore the potentiality of increasing the number of e^+ namely an extra RF field at the beginning of the capture section and a higher solenoidal field.

poirier@arronax-nantes.fr

1. Introduction

The CLIC positron source assumes unpolarised beams for the baseline configuration. A conventional scheme has been studied in [1], but, in order to reduce the beam energy deposition on the e^+ target converter, the concept of hybrid targets (Figure 1) has been adopted as the baseline for CLIC. A 5 GeV electron beam impinges on a crystal tungsten target aligned along its <111> axis. Photons produced via the channelling process go straight to an amorphous tungsten target while the charged particles are bent away, reducing the deposited energy. The tungsten target thickness is optimised for positron production [2,3].
This scheme allows a large number of photons to be produced per incoming electrons and thus with an optimised target a large number of positrons could be produced. The hybrid scheme parameters for the CLIC positron production are given in Table 1.
Downstream the amorphous target, an Adiabatic Matching Device (AMD) collects the positrons by reducing their transverse momentum. The Pre-Injector linac accelerates the positrons up to 200 MeV after which a bunch compressor reduces the bunch length and a conventional linac brings their energy to 2.86 GeV.

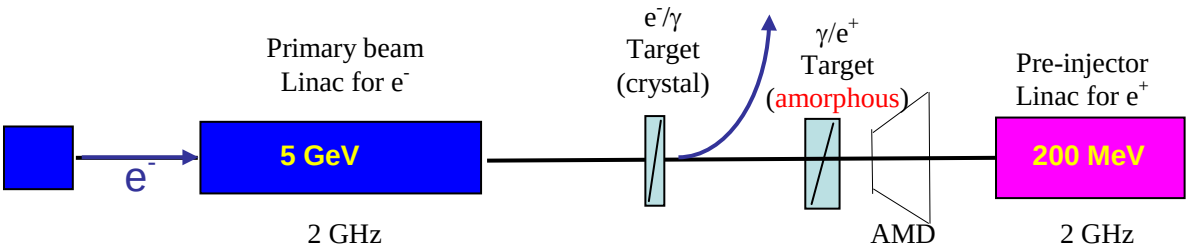

Figure 1 – Layout of the hybrid target scheme

Table 1: Hybrid target parameters

Parameters	Unit	Value
Incoming electron beam energy	GeV	5
Crystal target thickness	mm	1.4
Distance crystal – amorphous target	m	2
Amorphous target thickness	mm	10

The present studies are a continuity of a general studies on the CLIC positron source. Some of the studies have been performed on the AMD and Standing Wave (SW) cavities [4].

2. The capture and accelerating section

The capture and accelerating sections are constituted of the AMD and long Travelling Wave structures described below. Figure 2 shows the layout. These RF structures are embedded in a solenoidal field of constant amplitude 0.5T.

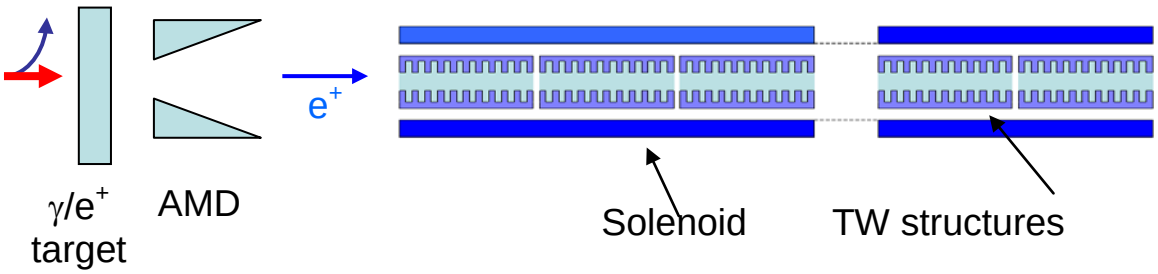

Figure 2 - Basic layout of the capture and accelerating sections

2.1. Capture section – Adiabatic Matching Device

The AMD is constituted of several coils, based on a slowly decreasing magnetic field and allows an improved e^+ yield having a wide momentum range acceptance. The present AMD is 20 cm long with a longitudinal magnetic field starting at 6 T and decreasing down to 0.5 T, which is the strength of the solenoid encapsulating the downstream accelerating section.
The parameters of the AMD are given in Table 2. The simulated inner aperture is a constant radius of 20 mm. It has to be noted that for the present positron energy spectrum, a shorter AMD helps to gather more particles (20 cm seems more favorable than 50 cm used in [2]).
A tapered inner aperture with a front face larger than 20 mm helps also to collect positrons.

Table 2: AMD parameters

Parameters	Unit	Value
Initial axial magnetic field	T	6
Final axial magnetic field	T	0.5
Length	mm	200
Vacuum chamber radius	mm	20

2.2 Travelling Wave accelerating section

The accelerating structures of the CLIC Pre-Injector linac studied here are Travelling Wave (TW), constant gradient (CG), 2π/3 mode, and room temperature technology. They are made of 84 copper cells and 2 couplers. This constitutes a full RF structure with a total length of 4.36 m as shown in Figure 2.

The geometry of the TW cells has been chosen to be pillbox in order to allow for a heat evacuation system as simple and efficient as possible. The TW structures are thus based on the SLAC type 2.856 GHz scaled to 2 GHz. The iris aperture for the TW is 20 mm.
The space between the structures is here 1 wavelength, i.e. 15 cm and can be increased (for pumping devices) to 2 wavelengths without particle loss.

The inner geometry and electric field are based for the following simulations, on studies performed with Superfish [6]. The beam dynamics simulation code ASTRA [7], used hereafter, employs the outputs of Superfish to describe by repetition the field and geometry of a full structure. A pillbox 4-cell cavity is the base for the construction of the travelling wave. The geometry of this cavity is given in Figure 3 and the electric field of the $2\pi/3$ mode is shown in Figure 4.
The pink dashed lines correspond to the repeated geometry and field, done 84/3=28 times. The two outer blue plain lines are the extremity of the 84 cells and can accommodates 2 couplers. For the simulation, the total field length L_T is based on:

$$L_T = N_c \times C_l + N_{co} \times C_{co} \times C_l + 2xD_l$$

where N_c=84 is the number of accelerating cell, C_l=0.0499 m is the cell length of the cavity, N_{co}=2 is the number of couplers, C_{co}=0.5 indicates that half of the couplers are filled with the electric field, and D_l=0.06m is the drift at each end of the structure .

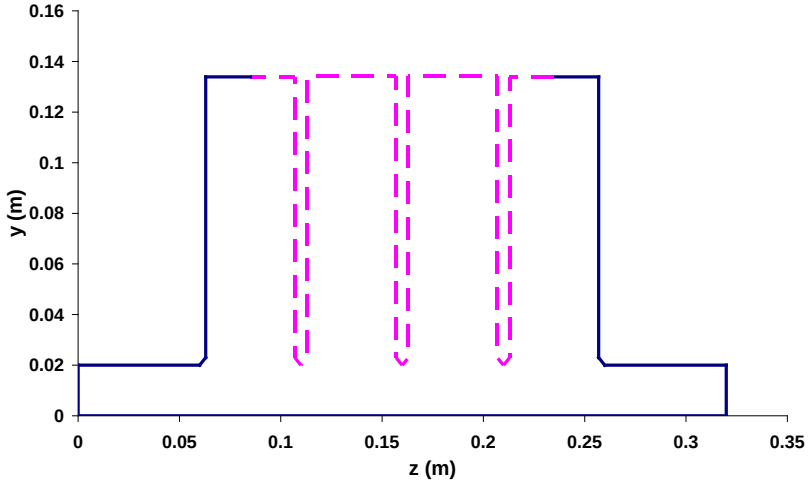

Figure 3 – The pillbox 4-cell cavity geometry as a base for the TW

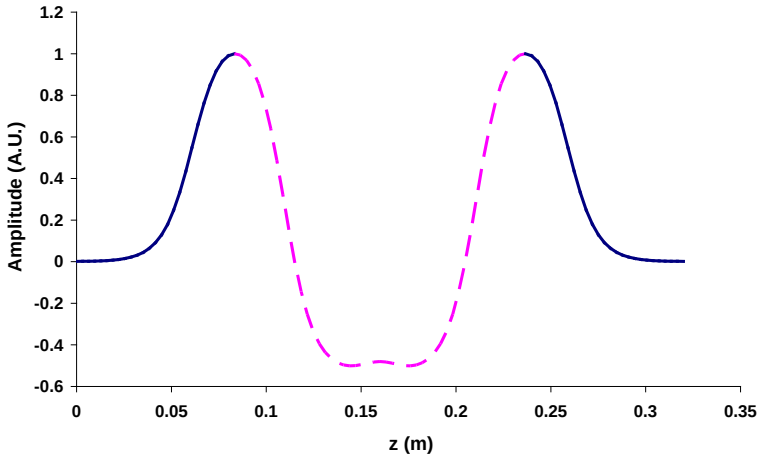

Figure 4 – Longitudinal electric field for the $2\pi/3$ mode travelling wave 4-cell cavity. The blue plain line is the couplers and drift fields, the pink dash line is the central electric field

Figure 5 shows the repetition of the central region of the 4-cell cavity (pink dash line). With this configuration the TW structure has a length of 4.36 m.
The maximum electric field is normalized to 1.

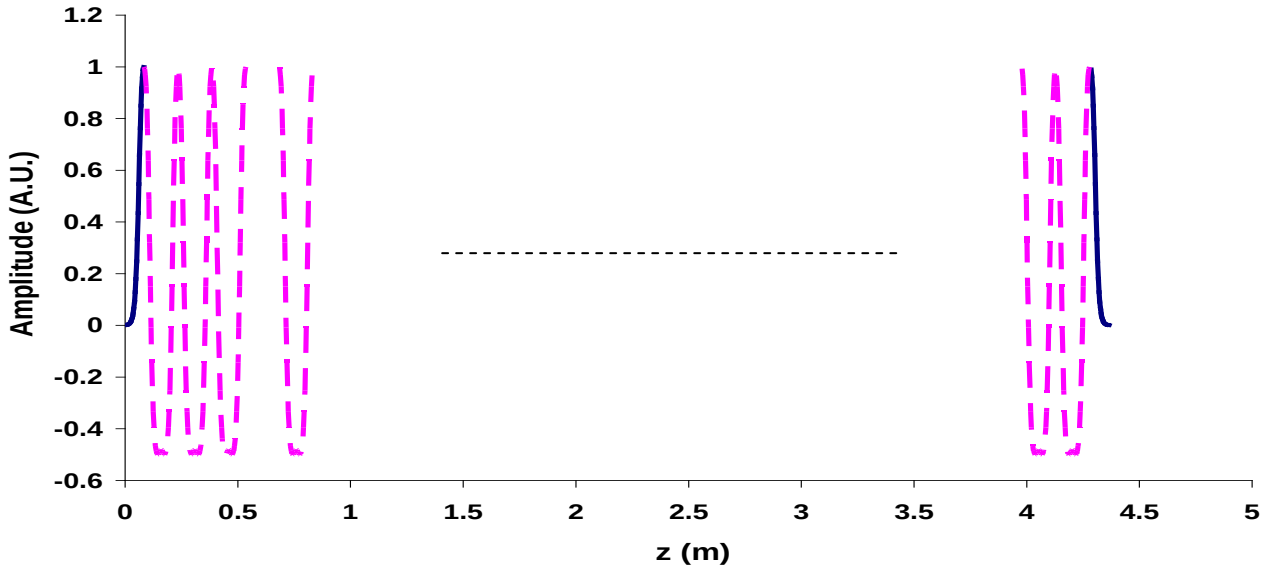

Figure 5 – Longitudinal electric field of the 2π/3 mode travelling wave

Table 3 summarizes the parameters of the TW structure for the CLIC Pre-injector linac.

Table 3 – Parameters of the accelerating structures

Parameters	Unit	Value
Length	m	4.36
Frequency	GHz	2
Nb of cells		84 + 2 couplers
Phase advance per cell		2/3π
Maximum Axial Electric Field	MV/m	15
Cell length	m	0.0499

3. Beam dynamics studies

Two modes of operation could be applied. The first one is based on acceleration of the positrons straight after the AMD. This mode has been used throughout the world on various accelerators and allows having a short accelerating section where the beam is boosted along the accelerating line.
The second one requires using the first accelerating structure in a decelerating mode such that a large number of positrons is captured. It is describe theoretically in [7]. In the following paragraph, the tuning necessary to implement these 2 modes with the corresponding results are given. .

For the TW sections used hereafter, the average energy of 20 particles at 100 MeV is shown in Figure 6. It indicates that the maximum acceleration occurs for a phase of 125^{o} and the

deceleration for a phase of 305°. It gives a good estimation for both modes of the RF phases to be used.

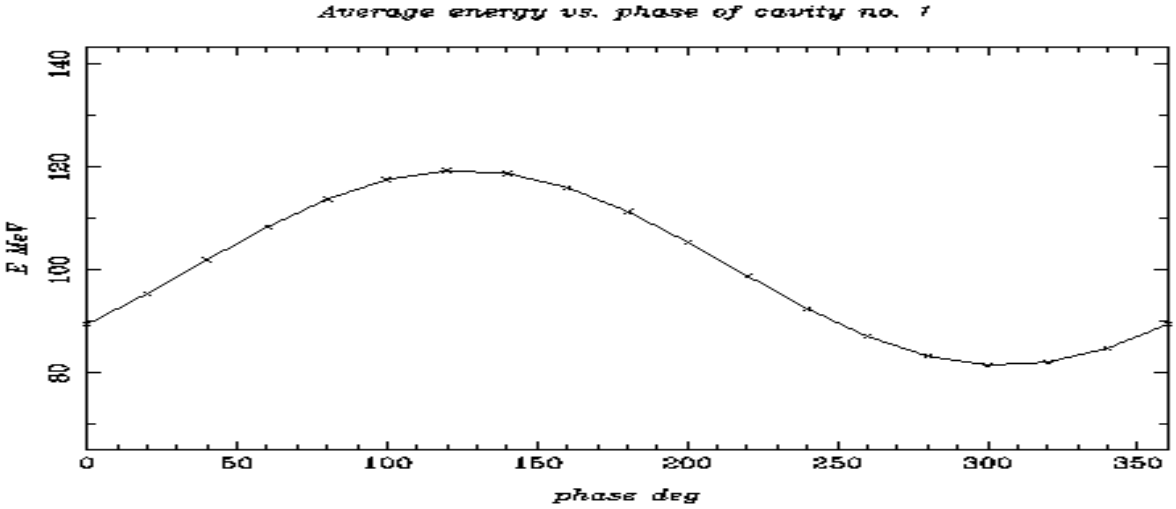

Figure 6: Mean energy versus RF phase

3.1. Accelerating phase results

As pointed out earlier for the accelerating mode the phase of the first section is tuned to perform maximum acceleration using the gradient available. Thus the phase is fixed at 120°, 5° lower than the maximum acceleration phase to cope with the length of the bunch. The phase of the following RF section is adjusted such that the head of the bunch is at the crest.

Figure 7 gives the energy of the positrons as a function of their position with respect to the reference particle (point 0 on the horizontal axis). The distribution is shown at 18.12 m downstream the 4th RF structure when accelerating mode is applied.

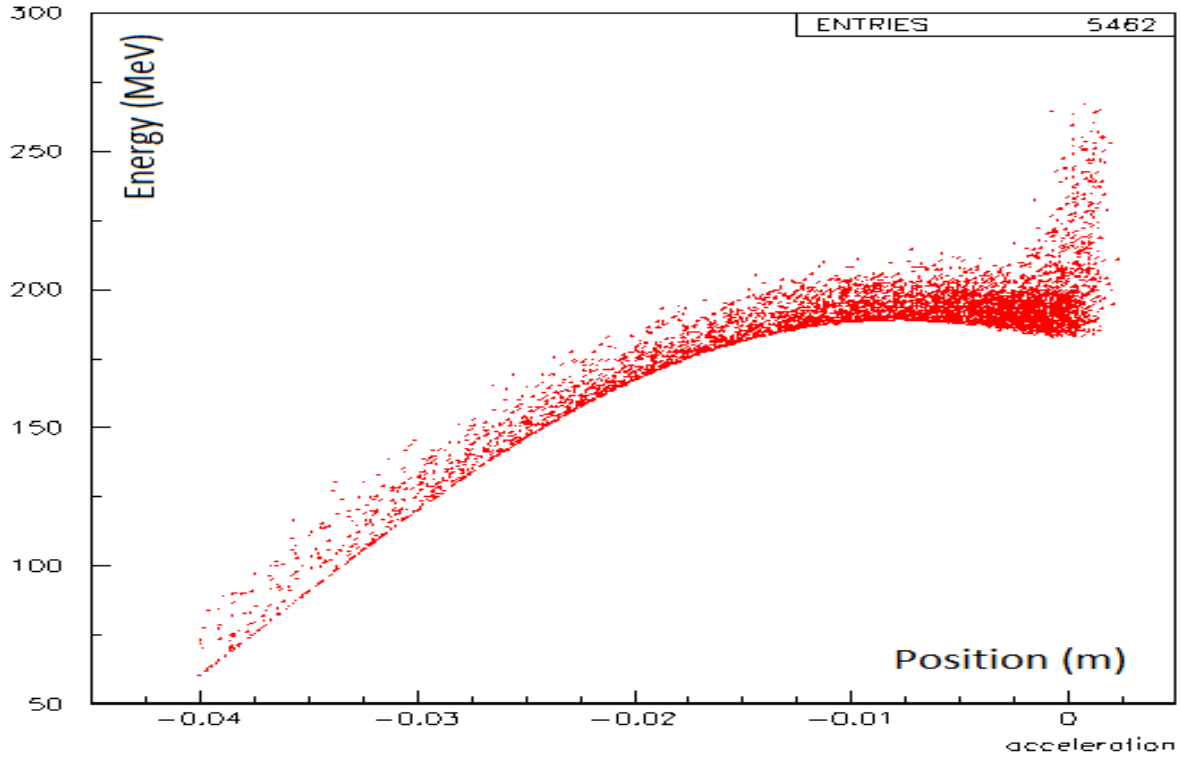

Figure 7: Energy distribution versus longitudinal position for the accelerating mode

.

It shows a concentration of particles at approximately 200 MeV and large longitudinal tail with particles extending up to 4 cm away of the reference one.

3.2. Decelerating phase results

3.2.1. Preliminary optimisation

The first optimisation is applied on the phase to perform the deceleration. In the present case, the RF phase is tuned at 280^{o}.
A second optimisation is applied on the gradient of the first section. This gradient has to be chosen in order to decelerate the particles strongly enough to obtain a grouping effect but also limited such that the positrons do not decelerate within the structure to their rest energy. If a too high gradient is used, positrons reaching the rest energy are then reaccelerated within the structure and their energy dispersion is increased at the end of the structure. A gradient of 6 MV/m is chosen for the first 2 GHz CLIC section and allows mitigating these effects. Figure 8 illustrates the longitudinal distributions at the end of the first section for several accelerating gradients.

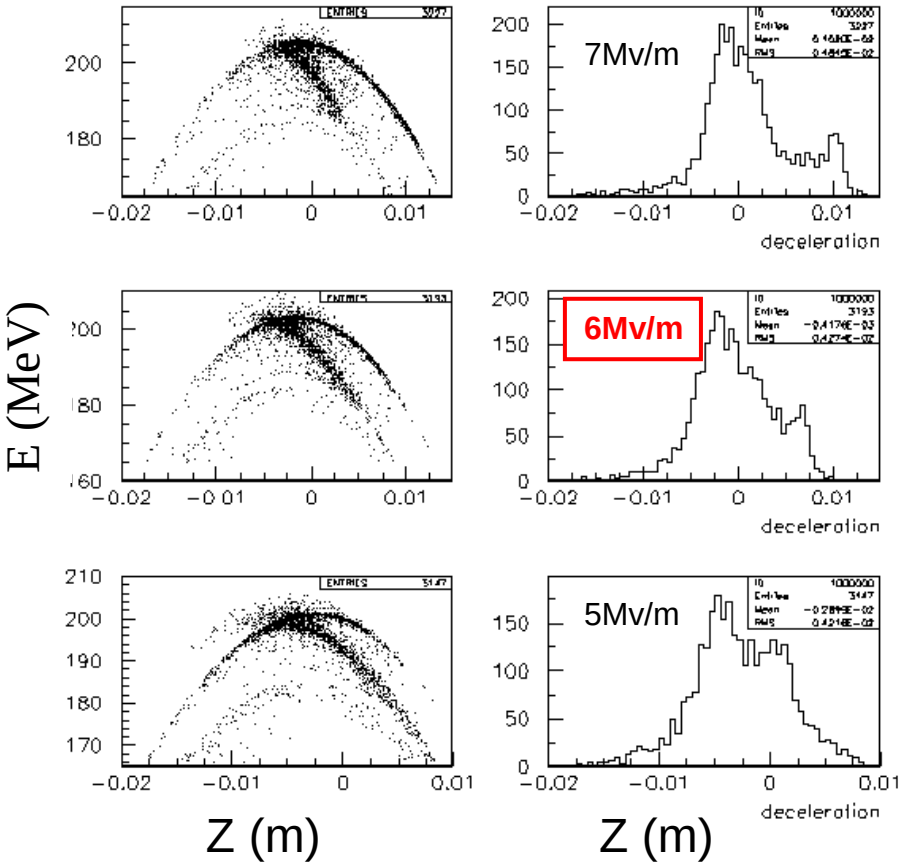

Figure 8: Longitudinal distributions at the end of the first section (phase 280^{o} and 3 peak gradients)

3.2.2. Results for decelerating mode

Figure 9 shows the energy of the positrons as a function of their position with respect to the reference particle when the decelerating mode is applied. The figure illustrates the results at the end of the last section at 22.63 m approximately. The positrons are confined in a small area around the reference particle and the energy dispersion is relatively constrained with a limited tail. Several upper tails appear in the right side of the reference particle denoting the deceleration process occurring in the first section. .

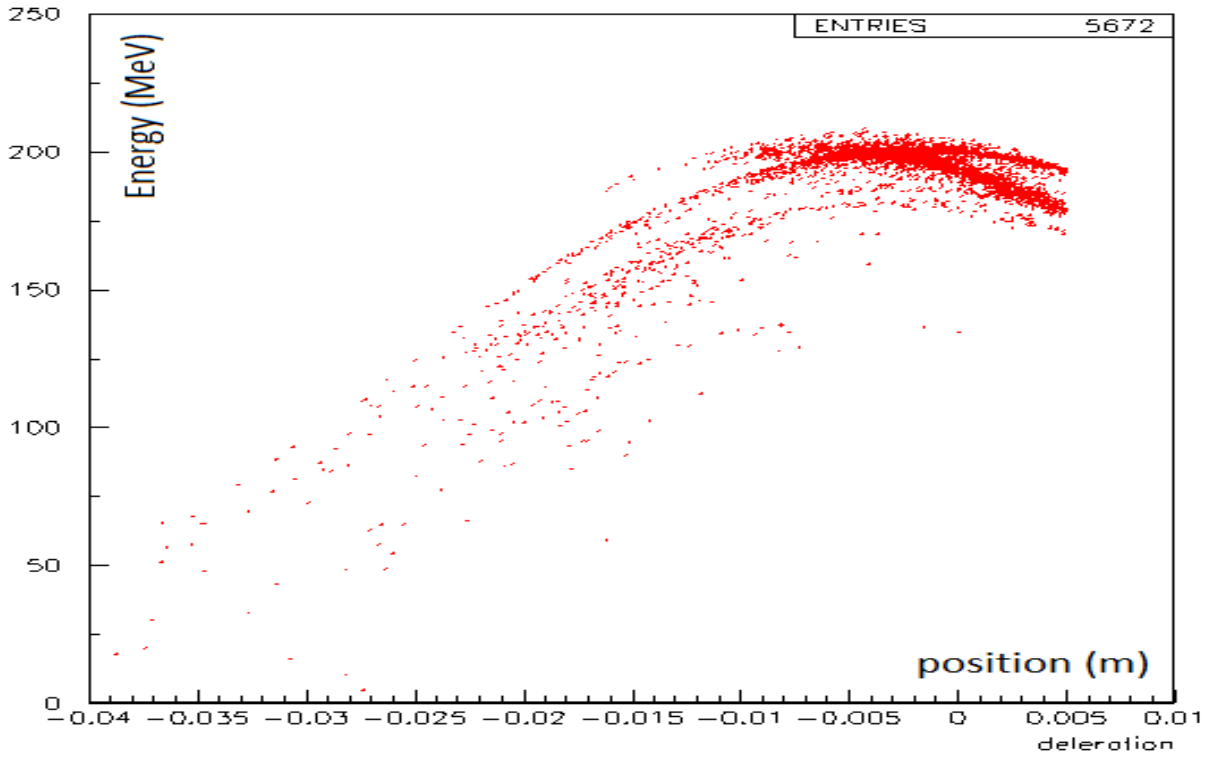

Figure 9: Energy distribution versus longitudinal position

3.3. Discussion

The total yield is defined as the number of positrons, at a given location (often the end of the embedded solenoidal field) over the number of electrons impinging on the crystal target.
The efficiency is defined as the total e^+ yield within a given window in energy. For the present simulations this window is 165 MeV < E < 300 MeV. These values are chosen assuming a Pre-Damping Ring energy acceptance of 1.2 %.
At the end of each of the accelerating and capture sections, the resulting total yield is slightly higher for the decelerating mode. The limiting factor is mainly the RF structure aperture which is identical in both cases. At a first glance, the main difference resides in the energy dispersion and bunch length. Table 4 gives the results for both modes.

Table 4: Comparison of accelerating and decelerating modes

Mode	Pre-Injector length (m)	Total yield	Efficiency	RMS bunch length (mm)	Mean Energy (MeV)	FWHM energy (MeV)	σ_x (mm)	$\sigma_{x'}$ (mrad)
Accelerating	18.12	0.9	0.77	9.54	191.8	10	8.06	2.86
Decelerating	22.63	0.95	0.89	4.37	197.5	4.5	7.83	2.86

The efficiency using the decelerating mode is 15% higher than using the accelerating one. This difference between each mode is even more explicit if the density of the particles is

plotted. Figure 10 illustrates the relative density plot of the positrons for both modes. In both cases, the number of positrons is given in a similar region of interest (windows of ± 5 MeV and ± 2.5 mm) around the highest density of positrons, assuming 15 mm for the iris radius. The decelerating mode shows 90% higher density, indicating that this technique maintains the positrons in a small confined area. This last point is important for the downstream acceleration limiting the energy dispersion due the bunch length dilution.

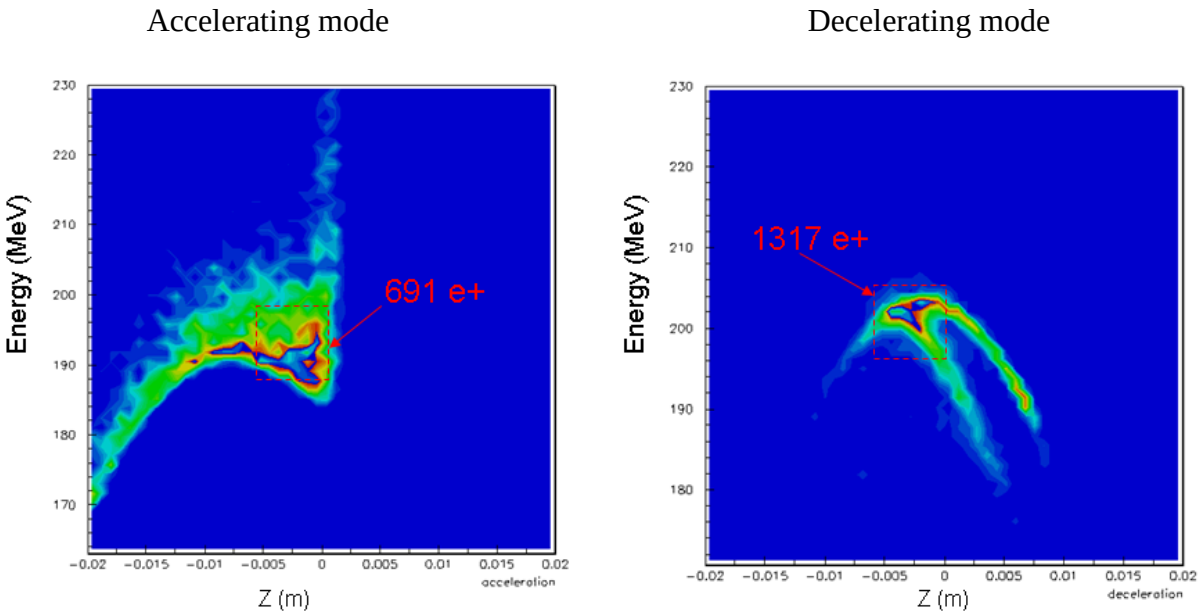

Figure 10: Density plot of the energy at 200 MeV

4. Impact of Space Charge

With the present bunch dimension at the exit of the target, the intensity of a bunch and the relativistic beam, the space charge effect was considered negligible in the previous sections. The space charge is time consuming when optimization of an entire accelerating line has to be done. Though when decelerating, the beam becomes less relativistic and space charge effect is more important than with full acceleration. In the following paragraph, the space charge effect is considered and a 10%-limit (level at which the space charge effect degrades by 10% the efficiency with respect to the level with no space charge) for each mode is checked. For the present beam intensity this study estimates the space charge effect on the positron yield. This helps also to get a margin to the 10% limit and indicates by how much the bunch charge has to be increased to get an efficiency reduction of 10%.

Figure 11 shows the results of the study for the accelerating mode and gives the efficiency of positrons capture at 200 MeV with respect to the number of particles in the bunch.
For a 10^{10} electrons i.e. ~1.6 nC per bunch, and 6000 simulated electrons, the charge per macro-particle is 2.7×10^{-4} nC. The space charge has been applied from the beginning of the AMD down to the last RF structure within the solenoid. Figure 11 illustrates the level with/without space charge and the level for a -10% effect.

For the accelerating mode, without space charge, the efficiency is approximately 0.77 and drops to ~0.75 when space charge for 10^{10} electrons is included. The impact of the space charge on the efficiency at the end of the 200 MeV, is a reduction of 3.6%.
An efficiency variation ΔE_f = -10% effect, i.e. an efficiency of 0.69, is reached when the charge per macro-particle is multiplied by 250 so in order to get a 10% effect, the total electron charge has to be multiplied by 250.

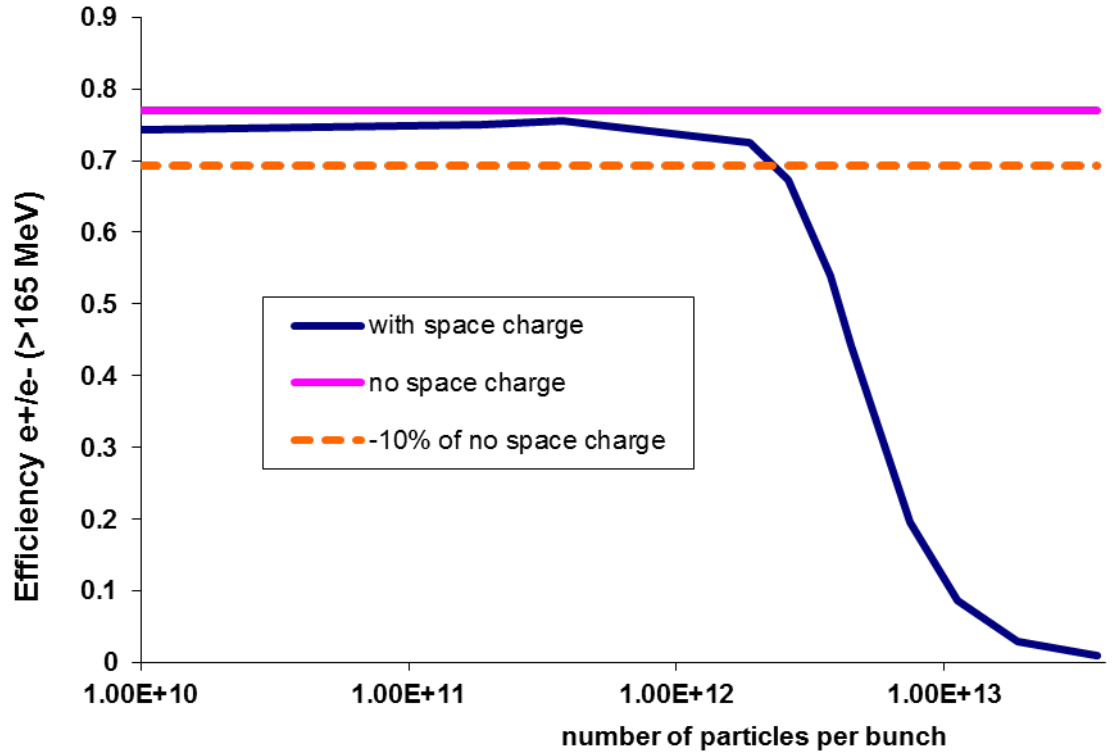

Figure 11: Efficiency of the capture at 200 MeV as a function number of particles per bunch.

For the deceleration, the efficiency is 0.89 and the impact of the space charge effect is approximately -4.6%, lowering the efficiency to 0.85. The expected charge at CLIC is 100 times lower than the charge which has a 10% effect.

In both cases, acceleration and deceleration, the study indicates that with the present bunch charge expected for the CLIC positron source, the space charge impact is negligible (lower than 5%) for the accelerating and capture section up to 200 MeV. A slight difference does exist between both cases, with a higher impact when deceleration is applied. These results support the idea of not using space charge effects when fast simulation is required for optimisation but also points out that details studies will require the inclusion of these effects.

5. Additional Studies

To explore the potential of increasing the efficiency at the end of the section, additional studies have been performed. These studies include the possibility to add an electric field within the adiabatic matching device and/or increase the magnetic field encapsulating the accelerating structures up to 200 MeV. These studies are presented below.

5.1. Stronger solenoid field

For the previous studies, the solenoid field is fixed at 0.5 T. An increased solenoidal field surrounding the RF sections will help to keep an optimum number of positrons. The following studies are performed to check the impact using field amplitude as high as 1 T. In this case, the AMD field decreases from 6 T down to 1 T.

5.2. Electric field superimposed to the AMD

A standing wave 4-cells cavity is used to accelerate the positrons within the AMD. It has an iris aperture of 20 mm. Figure 12 shows the layout of the Pre-Injector including the booster within the AMD. This could be made possible if the opening of the AMD is large enough to accommodate a cavity. These scenarios require further studies to investigate the experimental possibilities more precisely in view of superconducting AMD technology [8].

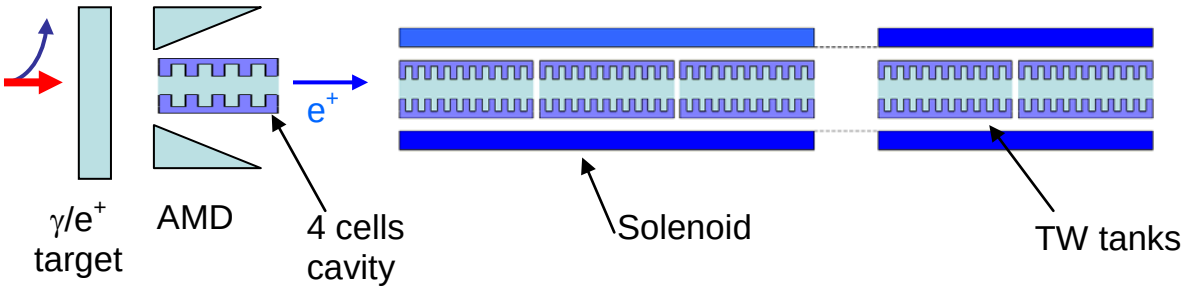

Figure 12: Layout of the accelerating capture section, including a standing wave 4-cell cavity within the AMD .

5.3. Results

The results of both additional scenarios are shown in Figure 13. A nominal case, with an AMD of 20 cm, 6T down to 0.5T and structure aperture of 15 mm, has been chosen as a reference here. The figure indicates the percentage increase of the number of positrons within a 12.5 mm z-window and 165-300 MeV energy window as a function of the cavity gradient within the AMD field. For an AMD without an RF structure, i.e. a cavity gradient of 0 MV/m, and an aperture of 20 mm (blue sky line), the results are proportional to the acceleration results obtained earlier for acceleration.

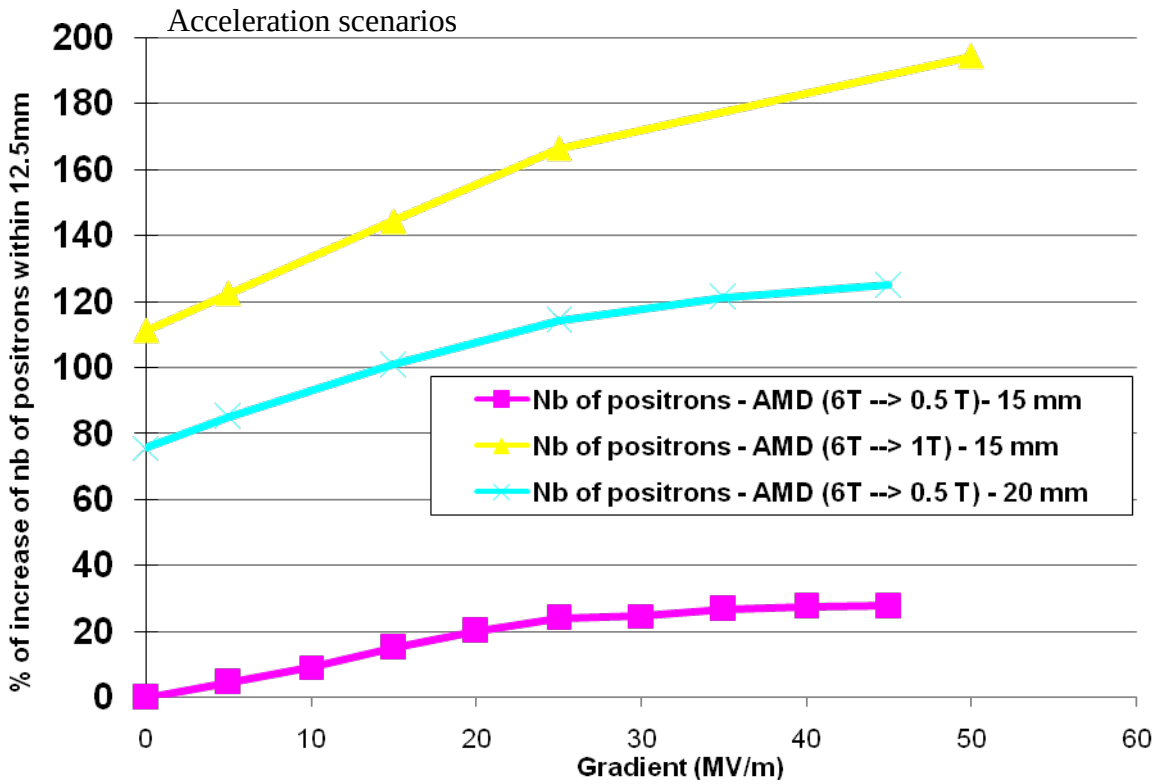

Figure 13: e+ increase versus gradient.

Figure 13 shows the impact of using larger aperture (i.e. from 15 mm to 20 mm). The increase of positrons is approximately 75%. The use of an AMD field going from 6T down to 1 T helps to gain ~110% when the aperture is 15 mm. This figure displays the linear increase of the gain of positron as a function of the cavity gradient. This increase is linear up to 25 MV/m and a cavity of 25 MV/m helps to gain approximately 30% of positrons with respect to the absence of cavity.

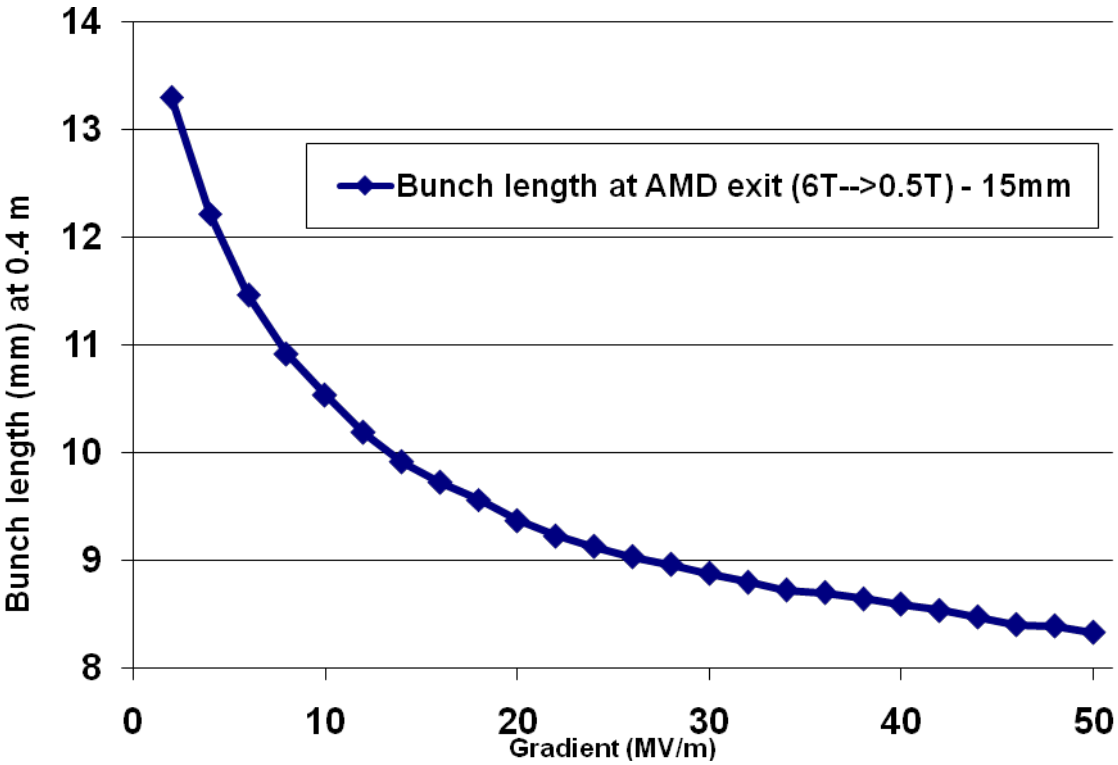

Figure 14 : Bunch length versus gradient at exit of 4-cell.

The relative gain of e^+ (or the decreased loss of e+) in Figure 13 is mainly due to a more compact bunch as the gradient increases. This is shown in Figure 14 with the bunch length at the end of the 4-cell cavity (0.4 m) versus the cavity gradient. The bunch length reduction also indicates that the energy dispersion will potentially be smaller at the end of the accelerating section and before the damping ring with higher inner cavity gradient. Theoretically, applying:

$$\frac{\Delta\gamma}{\gamma} \cong 1-\cos\frac{1}{2}\Delta\theta_{\infty} \cong \frac{1}{8}\left(\Delta\theta_{\infty}\right)^2$$

with $\Delta\theta_{\infty}$ the bunch rms length (in rad), the expected energy dispersion $\Delta\gamma/\gamma$ for an ideal and long accelerator can be calculated to be 4.3% for a bunch of 14 mm (cavity gradient = 0MV/m) and 1.4% for a bunch of 8 mm (cavity gradient = 50 MV/m). This latter result does not take into account transient RF, loading phenomena or precision and stability of cavity phasing.

6. Conclusion

For the CLIC positron source, the beam dynamics and positrons yield at 200 MeV have been studied for several scenarios. These studies are based on long TW structures and a short AMD. The study confirms that the deceleration technique for the RF structure downstream the AMD increases the yield. An optimisation of the phase in the RF structures is presented and the promising results for the decelerating mode are given.

Additionally, other scenaris are explored, mainly the inclusion of an extra electric field within the AMD and the use of a higher magnetic field along the Pre-Injector Linac. All these scenaris illustrate a potential increase of positron yield after the target. However they require further studies concerning the experimental possibilities. More precisely power consumption for the structures, beam loading effect and errors in the accelerating section (misalignments) need to be investigated. The power consumption of the TW structures will have a detrimental impact on the choice between SW and TW structures and futures studies should estimate the power requirements.

Further additional exploration could take into account possible scenaris based on deceleration and use of higher order modes accelerating structures.

7. Acknowledgments

The author would like to acknowledge the discussion with R. Chehab on the AMD particularly and V. Strakhovenko for the crystal target simulation.

8. References

[1] T. Kamitani, L. Rinolfi, “Positron production for CLIC”, CLIC note 465.

[2] O. Dadoun et al., “The Baseline Positron Production and Capture Scheme for CLIC”, presented at IPAC10, May 2010, CLIC-Note-824

[3] O. Dadoun et al., “Study of an Hybrid Positron Source using Channeling for CLIC”, CLIC-Note-808

[4] A. Vivoli *et al.*, “The CLIC e+ capture and acceleration in the Injector linac“, CLIC- Note -819

[5] "SUPERFISH - A Computer Program for Evaluation of RF Cavities with Cylindrical Symmetry", Particle Accelerators 7 (1976) 213-222

[6] K. Floettman, “Astra – A Space Charge Tracking Algorithm”, available at http://www.desy.de/~mpyflo/ .

[7] B. Aune and R. H. Miller, “New Method for positron production at SLAC”, LINAC1979, SLAC-PUB-2393.

[8] T. Omori, private communication, 2010